Stochastic Optimization for Distribution Grid Reconfiguration with High Photovoltaic Penetration

Andrej Trpovski*‡, Dante Fernando Recalde Melo*§, Thomas Hamacher†¶ and Tobias Massier*‖
*TUMCREATE, 1 CREATE Way, #10-02 CREATE Tower, Singapore 138602
†Technical University of Munich (TUM), Renewable and Sustainable Energy Systems, Garching 85748, Germany
‡andrej.trpovski@tum-create.edu.sg §dante.melo@tum-create.edu.sg
¶thomas.hamacher@tum.de ‖tobias.massier@tum-create.edu.sg

***Abstract*—Photovoltaics (PV) are considered as one of the most promising renewable energy source for Singapore. This paper proposes an optimization strategy for a distribution grid that includes PV. The objective is to provide optimal grid operation for seamless integration of distributed generation (DG). A novel approach for grid reconfiguration considering a probabilistic statistical model for the solar irradiance is introduced. A stochastic mixed-integer second order conic programming (SMISOCP) algorithm is devised to provide an optimal radial grid topology. The objective is to reduce power losses and operational costs of the grid. Case studies of grid model with distributed PV generators are conveyed to affirm the capability to deliver the objectives.**

***Index Terms*—Optimization, Smart Grids, Solar Power Generation, Power System Management, Quadratic Programming.**

NOMENCLATURE

Sets

Ω_l	Set of lines	
Ω_n	Set of nodes	
Ω_s	Set of substations	
H	Set of hours	
S	Set of scenarios	

Constants

Δh	Time frame	$[hour]$
γ	Switching cost	$[S\$/switching]$
ψ_h	Cost of electricity	$[S\$/kWh]$
$R_{i,j}$	Resistance of lines	$[\Omega]$
$X_{i,j}$	Reactance of lines	$[\Omega]$
$Z_{i,j}$	Impedance of lines	$[\Omega]$
$\overline{V}$	Maximum voltage magnitude	$[kV]$
$\underline{V}$	Minimum voltage magnitude	$[kV]$
$\overline{I}_{ij}$	Maximum current magnitude	$[A]$
$P^d_{i,h}$	Active power demand	$[kW]$
$Q^d_{i,h}$	Reactive power demand	$[kVar]$
$P^g_{i,h,s}$	Active power from PV generation	$[kW]$
$\zeta_{h,s}$	Probability of scenario s at hour h	
N	Number of scenarios	

Continuous variables

$I_{i,j,h,s}$	Current magnitude through lines	$[A]$
$V_{i,h,s}$	Voltage magnitude	$[kV]$
ν	Total cost excluding constant loads	$[S\$]$
$P^{grid}_{i,h,s}$	Active power supplied by the grid	$[kW]$
$P_{i,j,h,s}$	Active power flow through lines	$[kW]$
$Q^{grid}_{i,h,s}$	Reactive power supplied by the grid	$[kVar]$
$Q_{i,j,h,s}$	Reactive power flow through lines	$[kVar]$
$\omega_{i,j,h,s}$	Auxiliary variable used to model the state of the lines	

Binary variables

$\rho'_{i,j,h}$	Switching coefficient
$\rho_{i,j,h}$	Switch status of line ij

I. INTRODUCTION

The recent rapid advancement in telecommunication technologies, automation and information technologies give a broad perspective on smart grid development and implementation. The accelerated improvements in renewable energy generation technologies make intermittent power sources to be emphasized as the future of green power generation. Renewable sources of energy are an essential part of the future smart grid.

In the last decade, distributed generation (DG) is progressively implemented with significant increase in wind energy generation and solar energy generation capacities. With more than 227 GW solar energy generation capacities installed globally, their share in the global energy generation profile is more than ten times higher compared to 2009 [1]. By 2050, solar energy generation is estimated to take a share of 16 % of the global electricity generation [2]. In Singapore, 20 % penetration of solar energy generation in the electricity supply system is expected [3]. Having DG at the focus gives way to a new grid infrastructure, which brings certain challenges to the existing power system.

When considering PV for the optimization, obtaining a highly accurate solar irradiance point forecast is considered to be difficult and complex. Plenty of parameters need to be considered to perform a forecast [4]. The complexity of the methods depends on the instruments and data available to the forecaster, such as nearby meteorology stations and satellites, data on PV and numerical weather prediction models.

The majority of electricity generation is scheduled in the day-ahead market, thus a day-ahead point forecast is needed. This type of forecast is to be provided 18.5 to 42.5 hours prior to the operating day. With today's technology and approach, 24 to 48 hours ahead of time point forecast accuracy has a root mean square error in the range from 57 % up to 72 % [5]. Based on the mismatch between solar irradiance point forecast and the real solar irradiance values, uncertainty is one of the main challenges in distribution grids due to high PV penetration. This is not addressed with high accuracy when using the irradiance point forecast for a longer time period before the actual power generation.

Reconfiguration optimization is a method used for distribution grid optimization, being a topic of research for the past few decades. Progress has been slow and limited due to limitations in technology and cost. Recent development in remote supervision and control of technologically improved switch-breakers presents the opportunity to use efficient, economical and optimal reconfiguration methods. Many different methods are applied for distribution grid reconfiguration [6]. Loss reduction in the distribution grid can be addressed using heuristic rules to lessen the computational burden and reduce the number of iterations. However, the solutions obtained in this method are only approximate or local optimums [7]. Recently, artificial intelligence methods like particle swarm optimization, genetic algorithm or clonal selection algorithms are used [8], [9], [10]. Although these methods can provide major improvements and incorporate human reasoning to deal with the uncertainties in the distribution grid, global optimality is not guaranteed. Most recently, convex mixed-integer programming is used, which guarantees to have a global optimal solution [11], [12].

In this paper, reconfiguration is accomplished through transformation of the network topology. By operating the interconnection switch-breakers, the electrical behavior of the distribution grid is affected [13], [12]. A novel stochastic reconfiguration optimization method is presented with an objective to minimize the losses and operational costs. Different penetration levels of PV are considered. The solution must comply to maintain a radial topology and respect the voltage and current constraints [14]. By the use of constraints defined in the optimization, this reconfiguration method can also enhance the voltage profile, balance the load flow over the feeders and reinforce the grids reliability.

In Section II, a probabilistic model of the PV power output as an alternative to PV point forecast is presented. The network reconfiguration principle utilized through a novel SMISOCP, followed by a second order conic relaxation is defined in Section III. Case study to evaluate the method is conveyed and detailed in Section IV. In the last Section V, conclusion is derived.

II. Probabilistic Modeling of Photovoltaic Power Output

A. Addressing the Uncertainty with Probability Distribution Functions

In this paper, the irradiance point forecast is replaced by a probabilistic model obtained using statistical data. Solar irradiance is represented by a finite number of scenarios with an adequate probability. It is important to note that the quantity of statistical data available will affect the accuracy of the model and the final results.

The intermittent solar irradiance is modeled using probability distribution functions (PDFs) fitted from hourly statistical data. It is assumed that the hourly solar irradiance follows a bimodal distribution function as shown on Fig. 1. Linear combination of two unimodal PDFs using weighing coefficients is implemented to represent the bimodal PDF [15], [16]. The weighing coefficients W_1 and W_2 are obtained as follows

$$W_j = \frac{(number\ of\ samples)_{segment_j}}{(number\ of\ samples)_{total}} \qquad j \in 1,2$$

Different PDFs are fitted to the sectioned data, i.e., Weibull, Beta, Log-Normal and G. Extreme V. Theorem. To decide the best PDF fit to each section separately, Chi-squared and Kolmogorov-Smirnov goodness-of-fit tests are conveyed [17], [18]. A set of PDF plots fitted to a sample data for the time segment 15:00 - 16:00 during January is shown in Fig. 2.

Utilizing the goodness-of-fit test, p-values to evaluate the null hypothesis are obtained and compared with a significance level of 5 %. Although different fits show calculated probabilities good enough to confirm the null hypothesis for a single case, as seen in Fig. 2, the best fit is considered for greater accuracy. The results based on the Kolmogorov-Smirnov test are shown in Table I. According to Table I, the most common bimodal distribution in the peak hours follows Log Normal and G. Exreme Value PDFs defined by

$$\begin{aligned} f(x_i) = {} & W_1 \frac{1}{x_i\sqrt{2\pi\sigma_{l_i}^2}} \exp\left\{-\frac{\left[\ln(x_i)-\mu_{l_i}\right]^2}{2\sigma_{l_i}^2}\right\} \\ & + W_2 \frac{1}{\sigma_{g_i}}\left[1+\xi_i\left(\frac{x_i-\mu_{g_i}}{\sigma_{g_i}}\right)\right]^{(\frac{-1}{\xi_i})-1} \\ & \cdot \exp\left\{-\left[1+\xi_i\left(\frac{x_i-\mu_{g_i}}{\sigma_{g_i}}\right)\right]^{\frac{-1}{\xi_i}}\right\} \end{aligned} \tag{1}$$

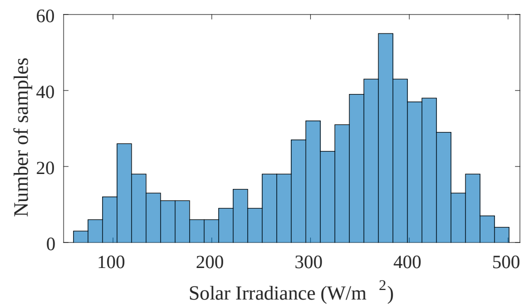

Fig. 1. Histogram of solar irradinace for 15:00 - 16:00 during January for period of 20 years.

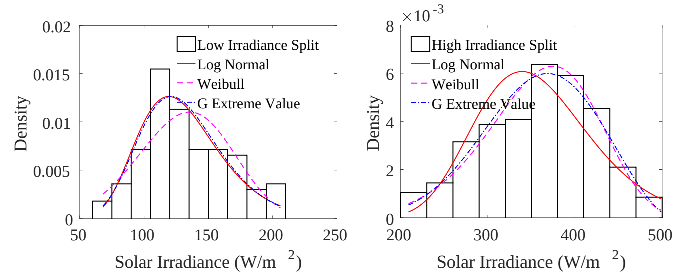

Fig. 2. PDFs fit on histogram for low and high irradiance segment for 16:00 in January.

TABLE I
KOLMOGOROV-SMIRNOV GOODNESS-OF-FIT TEST RESULTS FOR JANUARY

Hour	Low irradiance section	High irradiance section
09:00	Log-Normal	Log-Normal
10:00	Log-Normal	Weibull
11:00	G. Extreme Value	G. Extreme Value
12:00	Log-Normal	G. Extreme Value
13:00	G. Extreme Value	G. Extreme Value
14:00	Log-Normal	G. Extreme Value
15:00	Log-Normal	G. Extreme Value
16:00	Log-Normal	Weibull
17:00	Weibull	Log-Normal
18:00	Weibull	G. Extreme Value
19:00	Log-Normal	Weibull
20:00	Weibull	G. Extreme Value

In equation (1), x_i is the irradiance and $x_i > 0$; $W_j,\ j \in 1, 2$, is the weighing coefficient; σ_{l_i} is log standard deviation; μ_{l_i} is log mean; σ_{g_i} is scale parameter; μ_{g_i}, ξ_i are location and factor parameter respectively; i represent the hour of the day. For other cases of different unimodal distributions, the bimodal PDF is similarly defined.

Given the definition of solar irradiance distribution, the PV's power output used is described by

$$P_{PV} = E_e \cdot S_{PV} \cdot \eta_{PV} \tag{2}$$

In equation (2), P_{PV} is the power output (W); E_e is the solar irradiance (W/m^2); S_{PV} is the PV's installed surface (m^2); η_{PV} is the PV's efficiency.

B. Sampling

The irradiance is defined as continuous distribution function (CDF), meaning it is an infinite set of possible values along the specific distribution. Each of these values have a point probability equal to zero. For the bimodal distribution to be utile, it needs to be discretized with a finite set of scenarios. Monte Carlo sampling is used such that the CDF is approximated by a discrete set [19]. In this way, a finite and tractable scenario tree is constructed. The scenario tree contains N pairs of irradiance and probability values for each time segment when solar energy is available. Sampling is completed before optimization is performed.

III. NETWORK RECONFIGURATION

In order to represent the steady-state operation of the Electrical Distribution System (EDS), the following assumptions used for load flow formulation [13], [12], [20] are made:

- Electric loads are modelled as constant active and reactive power loads.
- The system is balanced and represented by its single-phase equivalent circuit.

The EDS notation is illustrated in Fig. 3. Consider EDS with a substation at node 0 and a meshed structure. It is assumed that all lines are equipped with switch-breakers that can open or close any feeder according to the configuration obtained.

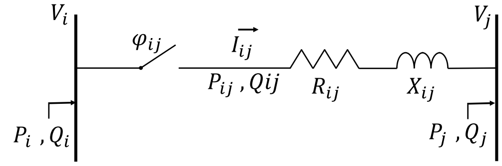

Fig. 3. Electrical Distribution System notation.

A. Stochastic Mixed-Integer Non-Linear Programming

The network reconfiguration optimization can be represented by a Mixed-Integer Non-Linear Programming (MINLP) formulation [11], [12]. All scenarios are considered in the optimization solution for each time segment. Doing this completely accounts the PV power output over the total period. Even though there are N different scenarios, the solution must provide a single optimal grid configuration for each time segment. Set S of scenarios and its probabilities $\zeta_{h,s}$, together with the set H of time segments for the total period analyzed are introduced. For simplified and more convenient notation, the following squared variables are introduced:

$$\upsilon_{i,h,s} = V_{i,h,s}^2 \qquad \text{and} \qquad \ell_{i,j,h,s} = I_{i,j,h,s}^2$$

A novel Stochastic Mixed-Integer Non-Linear Programming (SMINLP) optimization is defined as

$$\min_{\ell_{i,j,h,s}} \nu = \sum_{i,j\in\Omega_l} \sum_{h\in H} \sum_{s\in S} (\zeta_{h,s} \cdot R_{i,j} \cdot \ell_{i,j,h,s} \cdot \psi_h) + \sum_{i,j\in\Omega_l} \sum_{h\in H} \sum_{s\in S} \left(\rho'_{i,j,h} \cdot \gamma - \zeta_{h,s} \cdot P_{i,h,s}^g \cdot \psi_h\right) \tag{3}$$

subject to

$$P_{i,h,s}^{grid} + \sum_{j,i\in\Omega_l} P_{j,i,h,s} - \sum_{i,j\in\Omega_l} P_{i,j,h,s} - \sum_{i,j\in\Omega_l} [R_{i,j} \cdot \ell_{i,j,h,s}] + P_{i,h,s}^g = P_{i,h}^d \quad \forall i \in \Omega_n,\ h \in H, s \in S \tag{4}$$

$$Q_{i,h,s}^{grid} + \sum_{j,i\in\Omega_l} Q_{j,i,h,s} - \sum_{i,j\in\Omega_l} Q_{i,j,h,s} - \sum_{i,j\in\Omega_l} [X_{i,j} \cdot \ell_{i,j,h,s}] + Q_{i,h,s}^g = Q_{i,h}^d \quad \forall i \in \Omega_n,\ h \in H, s \in S \tag{5}$$

$$\upsilon_{i,h,s} - \upsilon_{j,h,s} = \omega_{i,j,h,s} + 2 \cdot R_{i,j} P_{i,j,h,s} + 2 \cdot X_{i,j} Q_{i,j,h,s} + Z_{i,j}^2 \ell_{i,j,h,s} \quad \forall i, j \in \Omega_l,\ h \in H, s \in S \tag{6}$$

$$|\omega_{i,j,h,s}| \leq \left|\overline{V}^2 - \underline{V}^2\right| \cdot (1 - \rho_{i,j,h}) \quad \forall i, j \in \Omega_l,\ h \in H, s \in S \tag{7}$$

$$\upsilon_{i,h,s} \ell_{i,j,h,s} = P_{i,j,h,s}^2 + Q_{i,j,h,s}^2 \quad \forall i, j \in \Omega_l,\ h \in H, s \in S \tag{8}$$

$$|P_{i,j,h,s}| \leq \overline{V}\,\overline{I}_{i,j} \rho_{i,j,h} \quad \forall i, j \in \Omega_l,\ h \in H, s \in S \tag{9}$$

$$|Q_{i,j,h,s}| \leq \overline{V}\,\overline{I}_{i,j} \rho_{i,j,h} \quad \forall i, j \in \Omega_l,\ h \in H, s \in S \tag{10}$$

$$0 \le \ell_{i,j,h,s} \le \left|\overline{I}_{i,j}\right|^2 \cdot \rho_{i,j,h} \qquad \forall i,j \in \Omega_l,\, h \in H, s \in S \quad (11)$$

$$|\underline{V}|^2 \le \upsilon_{i,h,s} \le \left|\overline{V}\right|^2 \qquad \forall i \in \Omega_n,\, h \in H, s \in S \quad (12)$$

$$\sum_{i,j \in \Omega_l} \rho_{i,j,h} = |\Omega_n| - |\Omega_s| \qquad \forall i,j \in \Omega_l,\, h \in H \quad (13)$$

$$\rho'_{i,j,h} \ge (\rho_{i,j,h+1} - \rho_{i,j,h}) \qquad \forall i,j \in \Omega_l,\, h \in H \quad (14)$$

$$\rho'_{i,j,h} \ge (\rho_{i,j,h} - \rho_{i,j,h+1}) \qquad \forall i,j \in \Omega_l,\, h \in H \quad (15)$$

The objective function in (3) is formulated to minimize the total cost of losses considering the switching costs and the PV generation revenue, while analyzing the full solar irradiance spectrum. Constraints (4) and (5) are used to assure power supply to each node and represent active and reactive power flow balance equations. Equation (6) is a function of the current magnitude and branch parameters along with the active and reactive power flow, which determines the voltage drop across connected lines. In equation (7), the auxiliary variable ω is defined to be zero when the line is connected, otherwise it can get any other value within the limits, to satisfy (6). Equation (8) calculates the current flow magnitude through the lines. Constraints (9) and (10) set the boundaries of the active and reactive power flow, while (11) and (12) limit the magnitude of the current flowing in the connected lines and the voltage at each node respectively. Equation (13) is defined to address the radiality of the network. However, this condition alone is not enough to guarantee the network's radiality. Together with constraints (4) and (5) both conditions are met and network radiality is guaranteed [21]. The switching status ρ and switching coefficient ρ' impose the binary representation of the optimization formulation. Constraints (14) and (15) are introduced to prevent negative values being assigned to the switching coefficient. Since single configuration per time segment is required, the last two constraints do not account for the different scenarios.

B. Second Order Conic Relaxation

A SMINLP optimization problem can not guarantee a convergence to global solution. With recent progress of advanced branch-and-cut technologies, mixed-integer conic solvers were developed. By the use of conic relaxation the optimization is made convex and convergence to optimality is assured.

In the optimization formulation, equation (8) is a non-convex constraint. Conic relaxation is performed by relaxing the quadratic equality as follows [22]

$$\upsilon_{i,h,s}\ell_{i,j,h,s} \;\ge\; P^2_{i,j,h,s} + Q^2_{i,j,h,s} \qquad \forall i,j \in \Omega_l\, h \in H, s \in S \quad (16)$$

which is equivalent to the conic representation

$$(2P_{i,j,h,s})^2 + (2Q_{i,j,h,s})^2 + (\ell_{i,j,h,s} - \upsilon_{i,h,s})^2 \;\le\; (\ell_{i,j,h,s} + \upsilon_{i,h,s})^2 \qquad \forall i,j \in \Omega_l\, h \in H, s \in S \quad (17)$$

By replacing (8) with (17) in the optimization formulation, a Stochastic Mixed-Integer Second Order Conic Programming (SMISOCP) problem is obtained. If the current $I^2_{i,j,h}$ through the lines is minimized, all constraints are met. The topology is radial and the original SMINLP is feasible, which assures that the solution of SMISOCP represents the global optimal solution [13].

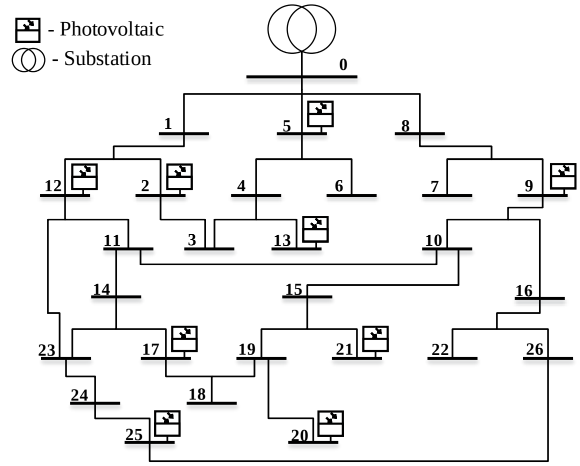

Fig. 4. Distribution grid model used for case study

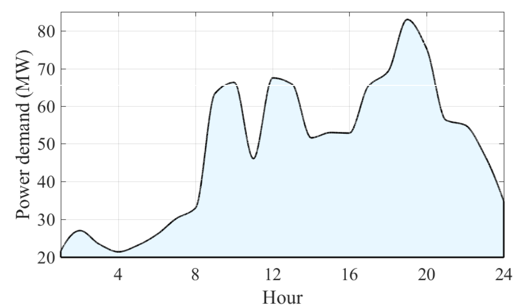

Fig. 5. Total load flow profile in the distribution grid used for case study

IV. Results and Analysis

A. Test System

The time segments used to address the proposed method are assigned intervals of 1 hour for a 24 hour period. A synthetic distribution grid network of 27 buses is used, having one substation and equally sized PV units connected to 9 nodes shown in Fig. 4. The PV units are sparsely distributed across the grid. Measurements of hourly load profiles of a real distribution grid in Singapore are used as load data for each node, shown in Fig. 5. The peak load of the distribution grid is 83 MW, for time segment 18:00 to 19:00. The method is assessed for different PV penetration levels from 0 - 100 % with a step size of 20 %. Total installed PV capacity for the case of 100 % PV penetration is set to match the peak load profile at 83 MW. Installed PV capacity for the rest of the cases is calculated accordingly. The probabilistic model used for the irradiance is obtained using statistical data for a period of 20 years. The irradiance data is sampled to 8 scenarios per hour. However, a single day of this data is considered for

TABLE II
COMPARISON OF NUMBER OF SWITCHING ACTIONS BEFORE AND AFTER INTRODUCING SWITCHING COST FOR 24 HOUR PERIOD

Switching cost	$\gamma = 0$	$\gamma = 50\%$	$\gamma = 100\%$
Number of switching actions	118	32	14

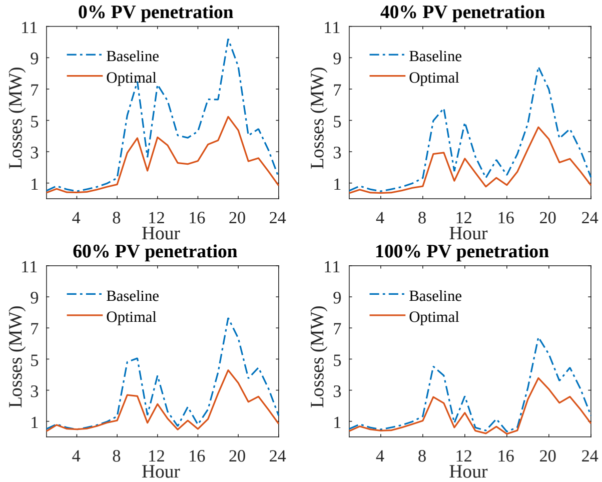

Fig. 6. Load flow study for grid's losses comparison for different cases

TABLE III
COST ANALYSIS COMPARISON FOR BASELINE AND OPTIMAL GRID CONFIGURATION STUDY CASES

	Losses(S$)		
Case	**baseline**	**optimal**	**loss reduction**
$0\% PV$	12895	7268	43.64%
$20\% PV$	10507	6003	42.87%
$40\% PV$	8668	4986	42.48%
$60\% PV$	7276	4369	39.95%
$80\% PV$	6262	3896	37.78%
$100\% PV$	5690	3489	38.68%

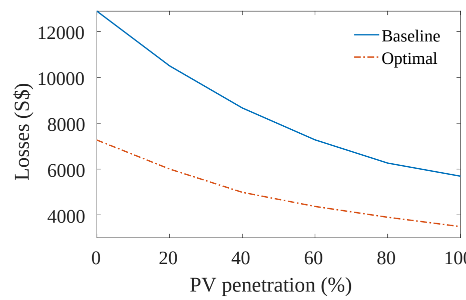

Fig. 7. Cost analysis of losses for different PV penetration level for baseline and optimal case studies

the comparison. According to the irradiance data, shown in Table I, the PV units are generating electricity input to the distribution grid between 08:00 and 20:00. Hourly electricity prices of a single day from Singapore's wholesale market are used for cost calculation.

The proposed method is being tested for hourly considered grid reconfiguration, which is not the current practice for grid operation. One of the reasons for having a rather limited change in the grid topology is the finite number of switching actions in the lifetime of the switching equipment, which is rather expensive. Therefore, the switching cost (γ) is introduced in the objective function, such that the proposed method can be considered for an economically efficient and practical application. Switching cost of a single switch action (γ) is calculated by summing an estimated price of a switch-breaker with installation costs adequate for Singapore. The sum is then divided by the maximum number of switching actions in the switch-breaker lifetime. By introducing the switching cost in the optimization, the number of switching actions is limited to a realistic applicable scenario. The number of switching actions is decided within the optimization such that a cost efficient operation is obtained, shown on Table II. Reducing the switching cost increases the number of switching actions for the tested period.

Two different sets with six cases each are developed. Set I is defined as a baseline set of cases for 0 - 100 % PV penetration, operated with a random radial network configuration. Set II consists of cases for 0 - 100 % PV penetration, operated with optimal radial network configuration.

B. Case Study Results

The SMISOCP optimization method is employed to reach optimal radial network configuration for Set II cases. A load flow study is then conveyed and analyzed. Each step of different PV penetration levels from Set II is compared to its equivalent case in Set I. Some of the results for different steps are shown on Fig. 6. Significant loss reduction can be noticed in all cases compared.

Since the loss minimization in the objective function is defined through cost minimization, comparison in cost of losses for all cases is conveyed for better evaluation of the method, shown in Table III. Analyzing the cost of losses for Set II compared to Set I demonstrates that the proposed method is very effective and the cost minimization objective is accomplished. The cost of the losses decreased from 37.8 % to 43.6 %. This can be considered as significantly large cost savings when an annual cost amount of the losses is considered.

Figure 7 and Table III can be observed to analyze the effect on cost of losses that different levels of PV penetration have on the distribution grid model used. By increasing the integration of PV generation, the losses decrease. When 100 % PV penetration is reached, losses decrease by 56 % and 52 % for the baseline and optimal scenarios when compared to the cases where no PV are present.

Even though PV with adequate design and placement can decrease the losses, solar intermittency is a big challenge for PV integration. Intermittent PV generation can result in changes in feeder voltage profiles, power quality issues regarding voltage fluctuations, frequent operation of voltage-control

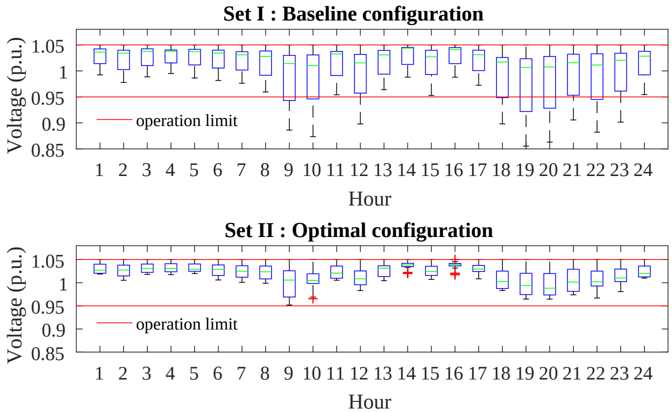

Fig. 8. Boxplot of hourly bus voltages for all buses for 80% PV penetration

TABLE IV
COMPUTATIONAL PERFORMANCE ANALYSIS FOR HOURLY OPTIMIZATION FOR 24 HOURS FOR APPROXIMATE AND OPTIMAL SOLUTIONS

	Approximate Solution		Optimal Solution	
Solving Time	**Time (s)**	**Opt_gap (%)**	**(s)**	**Opt_gap (%)**
average	2.34	0.68	18	0.01
minimum	0.3	0.84	4.4	0.01
maximum	15.9	0.25	60.8	0.01

and regulation devices, overcurrent and overvoltage protection issue and challenges regarding reliability and operation of the system [23]. Besides the main objective being loss reduction, the proposed optimization method has another benefit of addressing the voltage issues. It can enhance the voltage profile by limiting the voltage fluctuations, thus, smoothing the voltage peaks and drops. Enhancement in the voltage profile is reached for all levels of PV penetration for all analyzed cases. A single case result is shown in Fig. 8. Voltage profile enhancement provides better quality of power supply and more importantly, increases grid reliability and stability.

C. Computational Performance

The SMISOCP optimization is programmed in GAMS, using MOSEK as a solver [24]. The test is carried out on an Intel Core i7 CPU 2.60 GHz with 8 GB of RAM.

The computational performance of the optimization method is analyzed on a single hour reconfiguration, so that reference values for comparison to other available methods are obtained. Reconfiguration optimization is computed for each hour of the 24 hour period. An average solving time for a single-hour reconfiguration is obtained. The solving time can be significantly influenced by the level of accuracy, defined through the optimality gap tolerance [11]. The optimality gap represents the maximum distance to the global optimum solution. Default optimality gap for MOSEK to declare an integer solution as optimal is 0.01%. The approximate solutions are defined as the initial solutions obtained by the solver. The optimality gap for the initial solutions is in the range of 0.22 - 1.72 %. Table IV shows the computational performance analysis for both optimal and approximate solutions. The average solving time to obtain an initial solution is 2.34 sec with an average optimality gap of 0.68 %, which can be considered a very fast solution with great accuracy. In 77.08 % of the single hour reconfiguration cases, the solving time is under 1 sec. The optimal solution is obtained in average of 18 sec, with 70.83 % of the cases being solved under 20 sec, which can still be considered a fast solution for the reconfiguration problem.

Different time periods for grid reconfiguration can be used in the proposed method. However, the number of branches in the scenario tree created by the solver exponentially increases by increasing the analyzed reconfiguration period. Therefore, solving a period of 24 hours as a single reconfiguration problem requires excessive computational power. Hence, it is of practical interest that the 24 hour period is broken down into smaller periods, defined with respect to the complexity and size of the grid. In this way the optimal distribution grid configuration for the analyzed period of 24 hours can be reached in a more time-efficient way.

V. CONCLUSION

In this paper, we presented a stochastic optimization method through distribution grid reconfiguration. A probabilistic model of distributed PV generation was considered as an alternative to solar irradiance point forecast. A case study considering up to date grid data measurements, switching costs and prices was used to evaluate the proposed method. Analysis of the results show that the method is very effective and cost efficient. The proposed strategy provides optimal operation for the modern grids. Having cost effective operation of a grid as main priority, the method offers significant cost savings by notably reducing the losses. Different levels of PV penetration are analyzed, which gives a better picture of the potential of PV in future distribution grids. The optimization offers an operation of the grid within preset limits of the voltages and currents in all nodes and lines. This makes the model to be considered as a possible mechanism to enhance the voltage profile and control the feeder power flow. This method can offer improvements in grid reliability and stability, which is considered an essential step towards seamless integration of PV in the future smart grid.

VI. FUTURE WORK

The proposed method considers a different approach when compared to current practice of reconfiguration methods. This can influence the electrical behavior of the distribution system. Given the high dynamicity of configuration changes, the voltage stability is to be analyzed in depth through variety of voltage stability indices.

The method has proved to be very cost effective and time-efficient when tested on a small scale network. The complexity of the reconfiguration problem is to increase when real large distribution systems are considered. Future work is to estimate the cost benefits of loss reduction and the computational performance when dealing with large distribution grids. Different reconfiguration periods and optimality gaps are to be tested in order to find an appropriate setup of the reconfiguration optimization for grids with different complexity.

ACKNOWLEDGMENT

This work was financially supported by the Singapore National Research Foundation under its Campus for Research Excellence And Technological Enterprise (CREATE) programme.

REFERENCES

[1] G. Masson and M. Brunisholz, "2015 Snapshot of global photovoltaic markets," *Iea Pvps T1-29:2016*, pp. 1–19, 2016.

[2] J. Luther and T. Reindl, "Solar Photovoltaic (PV) Roadmap for Singapore," p. 75, 2013.

[3] International Energy Agency IEA, "Solar Photovoltaic Energy," Tech. Rep., 2014. [Online]. Available: http://bit.ly/1rHP5Kq

[4] K. Brecl and M. Topič, "Development of a Stochastic Hourly Solar Irradiation Model," *International Journal of Photoenergy*, vol. 2014, no. 2014, pp. 1–7, 2014.

[5] S. Pelland, J. Remund, J. Kleissl, T. Oozeki, and K. D. Brabandere, "Photovoltaic and Solar Forecasting: State of the Art," *International Energy Agency: Photovoltaic Power Systems Programme, Report IEA PVPS T14*, pp. 1–40, 2013.

[6] K. Kiran Kumar, N. Venkata Ramana, S. Kamakshaiah, and P. M. Nishanth, "State of Art for Network Reconfiguration," vol. 57, no. 1, 2013.

[7] T. Taylor and D. Lubkeman, "Implementation of heuristic search strategies for distribution feeder reconfiguration," *IEEE Transactions on Power Delivery*, vol. 5, no. 1, pp. 239–246, Jan 1990.

[8] S. Tuladhar, J. Singh, and W. Ongsakul, "A Multi-objective Network Reconfiguration of Distribution Network with Solar and Wind Distributed Generation using NSPSO," *International Conference and Utility Exhibition on Green Energy for Sustainable Development*, no. March, pp. 1–7, 2014.

[9] K. Nara, A. Shiose, M. Kitagawa, and T. Ishihara, "Implementation of Genetic Algorithm for Distribution Systems Loss Minimum Re-Configuration," *IEEE Transactions on Power Systems*, vol. 7, no. 3, pp. 1044–1051, 1992.

[10] A. Kavousi-fard and T. Niknam, "Optimal Distribution Feeder Recon fi guration for," *Ieee Transactions on Power Delivery*, vol. 29, no. 3, pp. 1344–1353, 2014.

[11] R. A. Jabr, R. Singh, and B. C. Pal, "Minimum loss network reconfiguration using mixed-integer convex programming," *IEEE Transactions on Power Systems*, vol. 27, no. 2, pp. 1106–1115, 2012.

[12] M. C. O. Borges, J. F. Franco, and M. J. Rider, "Optimal reconfiguration of electrical distribution systems using mathematical programming," *Journal of Control, Automation and Electrical Systems*, vol. 25, no. 1, pp. 103–111, 2014.

[13] J. C. López, M. Lavorato, and M. J. Rider, "Optimal reconfiguration of electrical distribution systems considering reliability indices improvement," *International Journal of Electrical Power and Energy Systems*, vol. 78, pp. 837–845, 2016.

[14] D. P. Bernardon, L. L. Pfitscher, L. N. Canha, a. R. Abaide, V. J. Garcia, V. F. Montagner, L. Comassetto, and M. Ramos, "Automatic reconfiguration of distribution networks using Smart Grid concepts," *2012 10th IEEE/IAS International Conference on Industry Applications*, pp. 1–6, 2012.

[15] M. Q. Wang and H. B. Gooi, "Spinning reserve estimation in microgrids," *IEEE Transactions on Power Systems*, vol. 26, no. 3, pp. 1164–1174, 2011.

[16] F. Youcef Ettoumi, A. Mefti, A. Adane, and M. Y. Bouroubi, "Statistical analysis of solar measurements in Algeria using beta distributions," *Renewable Energy*, vol. 26, no. 1, pp. 47–67, 2002.

[17] B. S. Borowy and Z. M. Salameh, "Optimum photovoltaic array size for a hybrid wind/PV system," *IEEE Transactions on Energy Conversion*, vol. 9, no. 3, pp. 482–488, 1994.

[18] Z. M. Salameh, B. S. Borowy, and A. R. A. Amin, "Photovoltaic Module-Site Matching Based on the Capacity Factors," *IEEE Transactions on Energy Conversion*, vol. 10, no. 2, pp. 326–332, 1995.

[19] M. Sovan, "A White Paper on Scenario Generation for Stochastic Programming," Tech. Rep. April, 2008.

[20] D. Shirmoharmnadi, H. W. Hong, A. Semlyen, and G. X. Luo, "A Compensation-Based Power Flow Method For Weakly Meshed Distribution and Transmission Networks," *IEEE Transactions on Power Systems*, vol. 3, no. 2, 1988.

[21] M. Lavorato, S. Member, J. F. Franco, S. Member, and M. J. Rider, "Imposing Radiality Constraints in Distribution System Optimization Problems," *IEEE Transactions on Power Systems*, vol. 27, no. 1, pp. 172–180, 2012.

[22] T. Ding, S. Liu, W. Yuan, Z. Bie, and B. Zeng, "A two-stage robust reactive power optimization considering uncertain wind power integration in active distribution networks," *IEEE Transactions on Sustainable Energy*, vol. 7, no. 1, pp. 301–311, 2016.

[23] F. Katiraei and J. R. Aguero, "Solar PV Integration Challenges," *IEEE Power And Energy Magazine*, vol. 9, no. 3, pp. 62–71, 2011.

[24] R. E. Rosenthal, *GAMS A User 's Guide*, 2016, no. January.

TABLE V
AUTHORS' BACKGROUND

Name	Title	Research Field	Personal website
Andrej Trpovski	PhD candidate	Smart Grid, Integration of Renewable Energy	http://bit.ly/2mvNyfj
Dante Fernando Recalde Melo	Research Fellow	Optimization of power system considering EVs and Renewable Energy	http://bit.ly/2lYAo7s
Tobias Massier	Principal Investigator	Electrification of bus lines and integration of electromobility into the grid	http://bit.ly/2mHtWSf
Thomas Hamacher	Full Professor	Renewable and Sustainable Energy Systems	http://bit.ly/2mHtWSf